

Electron-Rich Vaska-Type Complexes *trans*-[Ir(CO)Cl(2-Ph₂PC₆H₄COOMe)₂] and *trans*-[Ir(CO)Cl(2-Ph₂PC₆H₄OMe)₂]: Synthesis, Characterisation and Reactivity

Dipak Kumar Dutta,^{*[a]} Biswajit Deb,^[a] Bhaskar Jyoti Sarmah,^[a] J. Derek Woollins,^[b] Alexandra M. Z. Slawin,^[b] Amy L. Fuller,^[b] and Rebecca A. M. Randall^[b]

Keywords: Iridium / Phosphanes / Carbonyl ligands / Oxygen / Oxidative addition / Vaska's complex

The in-situ-generated dimeric precursor [Ir(CO)₂Cl]₂ reacts with four molar equivalents of the ligands 2-Ph₂PC₆H₄COOMe (**a**) and 2-Ph₂PC₆H₄OMe (**b**) to afford tetracoordinated complexes of the type *trans*-[Ir(CO)ClL₂] (**1a**, **1b**), where L = **a** and **b**. The IR spectra of **1a** and **1b** in CHCl₃ solution show the terminal ν(CO) bands at around 1957 and 1959 cm⁻¹, respectively, which are significantly lower in frequency compared to Vaska's complex, *trans*-[Ir(CO)Cl(PPh₃)₂] (1965 cm⁻¹) and substantiate the enhanced electron density at the metal centre. The single-crystal X-ray structure of **1a** indicates iridium–oxygen (ester group) distances [Ir⋯O(2) 3.24 Å, Ir⋯O(5) 3.29 Å] and angle [O(5)⋯Ir⋯O(2) 157.25°] suggesting a long-range intramolecular “second-

ary” Ir⋯O interaction resulting in a pseudo-hexacoordinated complex. Complex **1b** reacts with O₂ to generate [Ir(O₂)(CO)Cl(2-Ph₂PC₆H₄OMe)₂] (**2b**), while **1a** remains unreactive. Complex **2b** shows a distorted octahedral structure with peroxo O–O linkage (O2–O3 1.47 Å). The kinetic study of the reaction of **1b** and Vaska's complex towards dioxygen addition reveals that the rate of dioxygen addition to **1b** is about three times faster than Vaska's complex. Complexes **1a** and **1b** undergo oxidative addition with small molecules like CH₃I and I₂ to produce Ir^{III} carbonyl species of the type [Ir(CO)Cl(CH₃)IL₂] (**3a**, **3b**) and [Ir(CO)ClI₂L₂] (**4a**, **4b**), where L = **a**, **b**.

Introduction

Vaska's complex, *trans*-[Ir(CO)Cl(PPh₃)₂], occupies a central position of pivotal importance in the discovery of oxidative addition (OA) reactions of transition-metal complexes.^[1] The activation of small molecules such as CO, CH₃I, H₂, O₂, etc., by metal complexes^[2] is important and interesting due to their catalytic reactions; for instance oxidative addition of CH₃I is an important step in the rhodium-catalysed Monsanto^[3] and iridium-based Cativa^[4] process for acetic acid production. Activation of molecular oxygen by metal complexes has attracted great interest in recent years producing model oxidation catalysts for chemical processes in terms of cost, atom economy and the potential for limited by-products.^[2f,5] Vaska's discovery of the reversible molecular oxygen carrier^[6] [Ir(CO)Cl(PPh₃)₂] is of great importance, since the 1:1 oxygen adduct [Ir(O₂)(CO)Cl(PPh₃)₂] can be recrystallised and is extremely stable

and well characterised.^[7,8] The factors that influence these reactions have been the subject of much interesting discussion which has mainly been concerned with the electronic properties of the ligands.^[9–11] The importance of geometric aspects of the metal environment has also increasingly been recognised as evidenced by several publications in the last few decades.^[9,12,13]

The stereochemical properties of metal complexes depend mainly on the coordinating ligands as evidenced by the observation that some electronically similar iridium complexes show considerably different reactivities towards O₂, H₂ and other related molecules.^[12] The title compounds, *trans*-[Ir(CO)Cl(2-Ph₂PC₆H₄COOMe)₂] and *trans*-[Ir(CO)Cl(2-Ph₂PC₆H₄OMe)₂] in the present study are striking examples, in which the former complex has been found to be inert towards molecular oxygen at room temperature, while the latter is found to be about three times more reactive than Vaska's complex in oxygen uptake, although the physical properties of both complexes closely resemble Vaska's complex. As part of our continuing research activity,^[11,14] herein we report the structural and electronic characteristics of two new Vaska-type iridium complexes of P,O donor ligands, (2-Ph₂PC₆H₄COOMe) and (2-Ph₂PC₆H₄OMe), and their reactivity with small molecules such as O₂, CH₃I and I₂.

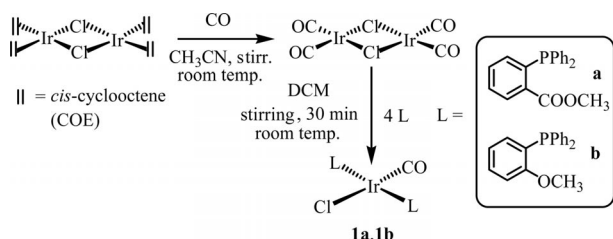
[a] Materials Science Division, Council of Scientific and Industrial Research, North-East Institute of Science and Technology, Jorhat 785006, Assam, India
Fax: +91-376-2370011
E-mail: dipakkrdutta@yahoo.com

[b] School of Chemistry, University of St. Andrews, St. Andrews, KY16 9ST, UK

Results and Discussion

Synthesis and Characterisation of **1a** and **1b**

In situ-generated dimeric precursor $[\text{Ir}(\text{CO})_2\text{Cl}]_2$ reacts with four molar equivalent of the ligands, L (**a**, **b**) by the cleavage of the chloro-bridge to afford tetracoordinated P-bonded complexes of the type *trans*- $[\text{Ir}(\text{CO})\text{ClL}_2]$ (**1a**, **1b**) (Scheme 1).



Scheme 1. Synthesis of **1a** and **1b**.

The observed elemental analyses data of the complexes agree well with their molecular composition. The IR spectra of **1a** and **1b** in nujol exhibit intense $\nu(\text{CO})$ bands at 1940 and 1942 cm^{-1} respectively, indicating the presence of terminal carbonyl groups. These νCO bands occur at significantly lower frequencies than those of the well-known Vaska's complex, (Table 1) and other related Vaska-type complexes^[12] like *trans*- $\{(\text{C}_6\text{H}_4\text{-2-CH}_3)_3\text{P}\}_2\text{Ir}(\text{CO})\text{Cl}$, *trans*- $\{(\text{C}_6\text{H}_4\text{-3-CH}_3)_3\text{P}\}_2\text{Ir}(\text{CO})\text{Cl}$ and *trans*- $\{(\text{C}_6\text{H}_4\text{-4-CH}_3)_3\text{P}\}_2\text{Ir}(\text{CO})\text{Cl}$. The low $\nu(\text{CO})$ values of **1a** and **1b** may be due to the formation of long-range intramolecular $\text{Ir}\cdots\text{O}$ secondary interactions by which the ester and ether oxygen atoms donate electron density to the metal centre, which in turn donates electron density to the antibonding π^* orbital of CO and consequently lowers the CO bond order. In order to obtain evidence for this intramolecular secondary interaction, the IR spectra of **1a**, **1b** and Vaska's complex were recorded in CHCl_3 solution where **1a** and **1b** exhibited intense terminal $\nu(\text{CO})$ bands at 1957 and 1959 cm^{-1} respectively, both frequencies being significantly lower than that recorded for Vaska's complex, 1965 cm^{-1} (Table 1).

Table 1. IR stretching^[a] of **1a**, **1b** and Vaska's complex, and their oxidative addition adducts.

Electrophiles	1a	1b	Vaska's complex
–	1940 ^[b]	1942 ^[b]	1952 ^[b]
	1957	1959	1965
CH_3I	2042	2040	2047
I_2	2063	2060	2067
O_2	–	2011	2015

[a] In CHCl_3 solution, unless otherwise stated. [b] In Nujol.

The ^1H NMR spectrum of **1a** shows a characteristic phenylic multiplet in the region $\delta = 7.34\text{--}8.21$ ppm and methyl singlet at $\delta = 3.47$ ppm. Similar to **1a**, **1b** also shows the phenylic multiplet in the range $\delta = 6.83\text{--}7.95$ ppm and methyl singlet at around $\delta = 3.59$ ppm. The appearance of upfield shifts of CH_3 protons compared to free ligands [$\delta = 3.73$ (**a**) and 3.72 (**b**) ppm] further substantiate the formation of $\text{Ir}\cdots\text{O}$ bonds. $^{31}\text{P}\{^1\text{H}\}$ NMR spectra of **1a** and **1b**

show characteristic downfield shifts at $\delta = 29.0$ and 19.5 ppm compared to their corresponding free ligands $\delta = -3.71$ (**a**) and -16.13 (**b**) ppm. ^{13}C NMR spectra of **1a** show terminal CO resonance at $\delta = 181.3$ ppm, and the chemical shifts due to the phenylic and methyl carbon atoms are found in the range $\delta = 126.3\text{--}135.8$ and 51.76 ppm, respectively. Similar to **1a**, the ^{13}C NMR spectrum of **1b** also exhibits the characteristic resonance of terminal CO at around $\delta = 180.1$ ppm, and the resonance due to the phenyl and methyl carbon atoms are found in the range $\delta = 123.3\text{--}138.6$ and 55.73 ppm, respectively.

The crystal structure of **1a** (Figure 1, Tables 2 and 3) reveals that the iridium atom lies in an approximately square-planar environment formed by the two phosphorus donors, Ir, C (of CO) and Cl atoms. The ester carbonyl oxygen atom of the two phosphane ligands points towards the iridium centre from above and below the vacant axial sites of the

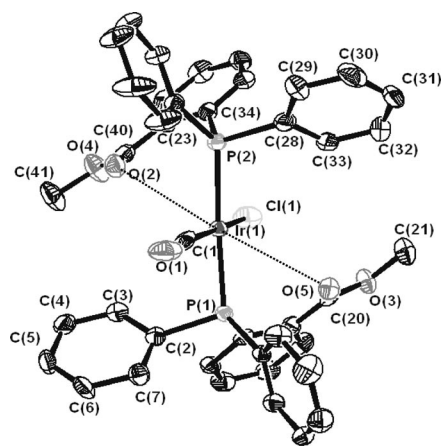


Figure 1. X-ray crystal structure of **1a**. Hydrogen atoms are omitted for clarity.

Table 2. Summary of X-ray single-crystal data and structure refinement parameters for **1a** and **2b**.

	1a	2b
Empirical formula	$\text{C}_{41}\text{H}_{34}\text{ClIrO}_5\text{P}_2$	$\text{C}_{40}\text{H}_{36}\text{Cl}_3\text{IrO}_5\text{P}_2$
Crystal colour	Yellow	Orange
Molecular mass	896.34	957.25
Temperature [K]	125	125
Crystal system	monoclinic	triclinic
Space group	$P2_1/n$	$P\bar{1}$
a [Å]	14.6003 (10)	9.8000(6)
b [Å]	16.8562 (9)	10.5916(17)
c [Å]	14.7687 (10)	19.381(3)
α [°]	90	79.736(15)
β [°]	70.483(2)	79.570(18)
γ [°]	90	76.321(17)
Z	4	2
Volume [Å ³]	3529.8(4)	1903.0(3)
$\rho_{\text{calcd.}}$ [g cm ⁻³]	1.687	1.549
λ [Å]	0.71075	0.71075
μ [mm ⁻¹]	4.005	3.778
$F(000)$	1776.0	878.0
$\theta_{\text{max.}}$ [°]	26.37	26.37
Reflections collected	7013	7548
R (obsd. data)	0.0324 (6663)	0.0685(6956)
wR_2 (all data)	0.1265 (7013)	0.1952(7548)

planar complex. The spectroscopic evidence (FTIR and ^1H NMR spectroscopic data) as well as the observed iridium–oxygen distances [Ir(1)⋯O(2) 3.246 Å; Ir(1)⋯O(5) 3.290 Å] (sum of the van der Waals radius of Ir–O \approx 3.52 Å) indicate long-range intramolecular “secondary” Ir⋯O interactions leading to a pseudo-hexacoordinated complex. A similar type of long-range interaction was earlier reported by us^[11] for a rhodium complex of the 2-Ph₂PC₆H₄COOMe ligand, where the Rh⋯O distances were 3.08 and 3.18 Å. Another long-range interaction was earlier reported for a palladium complex of 2-phenyl phosphanyl anisole, where the Pd⋯O distance was 3.17 Å.^[15] Miller and Shaw also indicated a typical long-range interaction for the complex *trans*-[Ir(CO)Cl{PMe₂(2-MeOC₆H₄)₂}₂] in which an Ir⋯O “secondary” bond with the methoxy oxygen was reported.^[16]

Table 3. Selected bond lengths [Å] and bond angles [°] of **1a** and **2b**.

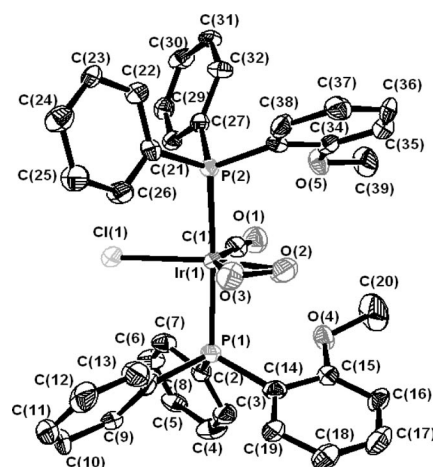
1a		Bond lengths	
P1–Ir1	2.3174(16)	P2–Ir1	2.3360(16)
C11–Ir1	2.3670(13)	C1–Ir1	1.903(5)
C1–O1	0.972(7)	Ir1⋯O2	3.24
Ir1⋯O5	3.29		
Bond angles			
P2–Ir1–P1	177.13(4)	C1–Ir1–C11	172.69(15)
Ir1–C1–O1	175.1(5)	O5⋯Ir1⋯O2	157.25
2b		Bond lengths	
P1–Ir1	2.354(3)	P2–Ir1	2.356(3)
C11–Ir1	2.412(3)	C1–Ir1	1.883(12)
C1–O1	1.134(13)	O2–O3	1.469(12)
O2–Ir1	1.994(8)	O3–Ir1	2.047(8)
Bond angles			
C1–Ir1–O2	109.4(4)	C1–Ir1–O3	152.0(4)
O2–Ir1–O3	42.6(3)	P1–Ir1–P2	172.06(8)
C1–Ir1–C11	96.9(4)	O1–C1–Ir1	172.8(10)
O3–O2–Ir1	70.6(5)	O2–O3–Ir1	66.8(5)

Reactivity of **1a** and **1b** with Molecular Oxygen

An interesting characteristic of square-planar Ir^I complexes is that they bind O₂ reversibly through side-on bonding. However, the stereochemical behaviour of the Ir centre is affected by the presence of different coordinating ligands. In the present investigation, complex **1a** is found to be unreactive towards dioxygen, even after prolonged treatment with O₂. The reactivity of **1a** was also tested under harsh conditions, i.e. in the temperature range 50–100 °C and O₂ pressure 5–10 bar, in an autoclave using toluene as solvent. Under these conditions, only 5–8% dioxygen adduct was detected spectroscopically. The dioxygen adduct was found to be stable only in solution. The lack of reactivity of **1a** may be due to the steric effect of the ligand 2-Ph₂PC₆H₄COOMe as revealed by the crystal and molecular structure of **1a** (Figure 1). The two COOCH₃ groups, one from each phosphane, are located near the apical positions [Ir(1)⋯O(2) 3.246 Å; Ir(1)⋯O(5) 3.290 Å] of the planar *trans*-[Ir(CO)ClP₂] unit, which may effectively protect the central iridium atom from the attacking molecular oxygen.

Such steric inhibition towards dioxygen addition was also reported by Vaska and co-workers^[6b,12] for the complex *trans*-[{(C₆H₄-2-CH₃)₃P]₂Ir(CO)Cl], in which the steric effect caused by –CH₃ groups was explained with the help of both molecular models and a single-crystal X-ray structure determination.

On the other hand, complex **1b** was found to be very reactive towards dioxygen and even more reactive than Vaska's complex. It is interesting to note that the related complex *trans*-[{(C₆H₄-2-CH₃)₃P]₂Ir(CO)Cl] shows no activity towards dioxygen^[6b,12] although both complexes have similar configuration apart from their *ortho* substituents. In order to explain the origin of such completely different behaviours of the title complexes, one should consider a few points which might alter the reactivity of the central metal atom.^[17] For complexes of the same metal, reactivity is increased by strong σ -donor and polarisable ligands. Partial and total deactivation is caused by strong π -acceptor ligands or electronegative ligands or a positive charge on the complex. In addition to the above electronic factors, steric effects of the ligand environment also have a profound influence on the reactivity of the metal centre.^[12,17,18] The inertness of **1a** towards O₂ addition may be caused by the strong steric influence of ligand **a** as demonstrated (vide supra). However, in order to substantiate the significantly high reactivity of **1b**, one should consider the combined effect of electronic as well as steric factors of the ligand. The higher electron density of the metal centre influenced by the OCH₃ group of **b** may enhance the susceptibility of the central metal atom towards dioxygen addition. In respect of the steric effect of **b**, it is likely that during dioxygen addition, the Ph₂PC₆H₄-2-OCH₃ ligands may rotate and readjust in such a way that the incoming molecules suffer less steric hindrance. This may be partially substantiated by the observed Ir⋯OCH₃ spatial distances [O(5)⋯Ir(1) 3.546 Å, O(4)⋯Ir(1) 3.551 Å, C(39)⋯Ir(1) 4.563 Å, C(20)⋯Ir(1) 4.409 Å] as obtained from the X-ray crystal structure of **2b** (Figure 2).

Figure 2. X-ray crystal structure of **2b**. Hydrogen atoms and uncoordinated solvent molecules are omitted for clarity.

It is interesting to mention here that attempts to develop single crystals of **1b** in CH_2Cl_2 or in any other solvent in air result in the formation of dioxygen adduct $[\text{Ir}(\text{O}_2)(\text{CO})\text{Cl}(2\text{-Ph}_2\text{PC}_6\text{H}_4\text{OMe})_2]$ (**2b**), which indicates that **1b** is very susceptible to dioxygen addition when it is kept in solution, however, it is very stable in the solid state for a longer period. The dioxygen adduct **2b** has been characterised by elemental analysis, IR, NMR and single-crystal X-ray diffraction. The appearance of IR bands at around 2011 and 858 cm^{-1} indicate the presence of CO and O–O groups, respectively, in the compounds. The ^1H NMR spectrum of **2b** shows the chemical shift for the $-\text{OCH}_3$ group at around 3.71 ppm which is closer to the $-\text{OCH}_3$ shift of the free ligand [^1H NMR (CDCl_3): $\delta = 3.72$ (**b**) ppm] indicating that the iridium–oxygen secondary interaction disappears after O_2 addition (Figure 3). The single-crystal X-ray structure of **2b** (Tables 2 and 3, Figure 2) reveals that the iridium atom lies in a distorted octahedral environment formed by the two phosphorus donors, O–O (peroxo), C (of CO) and Cl atoms. The O–O [O2–O3 1.469(12) Å] and Ir–O [O2–Ir1 1.994(8) Å, O3–Ir1 2.047(8) Å] bond lengths, and O–Ir–O [O2–Ir1–O3 42.6(3)°] bond angle in **2b** are similar to the Vaska dioxygen adduct reported by Lebel et al.^[8]

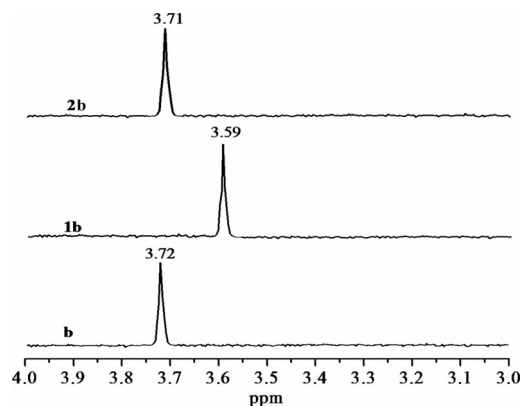


Figure 3. ^1H NMR spectra of **b**, **1b** and **2b** show the significant chemical shifts of $-\text{OCH}_3$ protons.

The rate of reactivities of **1b** and Vaska's complex towards O_2 addition were monitored by both UV/Vis and IR spectroscopy. Figure 4 shows a typical series of UV/Vis spectra for the reaction of **1b** with O_2 at $25\text{ }^\circ\text{C}$, in which the bands appearing in the visible ($\lambda_{\text{max}} = 434.5, 382.5\text{ nm}$) and near-visible ($\lambda_{\text{max}} = 331.4\text{ nm}$) region undergo decay until equilibrium is attained. The appearance of an isosbestic point close to the peak 331.4 nm indicates that the O_2 uptake reaction is proceeding without forming an intermediate or multiple products.

An absorbance vs. time plot for the decay of λ_{max} 382.5 nm is shown in Figure 5a. A linear fit of pseudo-first order was observed for the entire course of the reaction of O_2 with **1b** as is evidenced from the plot of $\ln(A_0/A_t)$ vs. time, where A_0 and A_t are the absorbance at time $t = 0$ and t , respectively (Figure 5b). From the slope of the plot, the rate constant was calculated and found to be $2.53 \times 10^{-3}\text{ s}^{-1}$.

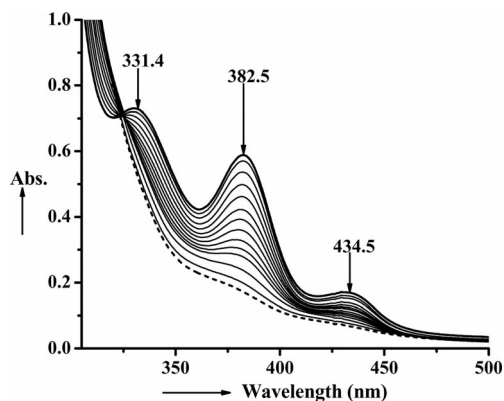


Figure 4. Series of UV/Vis spectra illustrating the reaction of **1b** with molecular O_2 at $25\text{ }^\circ\text{C}$. The arrows indicate the behaviour of each band as the reaction progresses.

In order to check the correctness of the experimental rate constant as obtained from UV/Vis spectroscopy, similar kinetic experiments were carried out using FTIR spectroscopy by monitoring the changes in the $\nu(\text{CO})$ bands with known concentration of **1b** as used in UV/Vis spectroscopy. In this experiment, when **1b** reacts with O_2 in toluene as solvent at $25\text{ }^\circ\text{C}$, an IR band appears at around 1955 cm^{-1} which then decays with a new band appearing at 2010 cm^{-1} which finally replaces the former band. A plot of $\ln(A_0/A_t)$ vs. time indicates a pseudo-first-order reaction in which the rate constant was found to be almost the same as

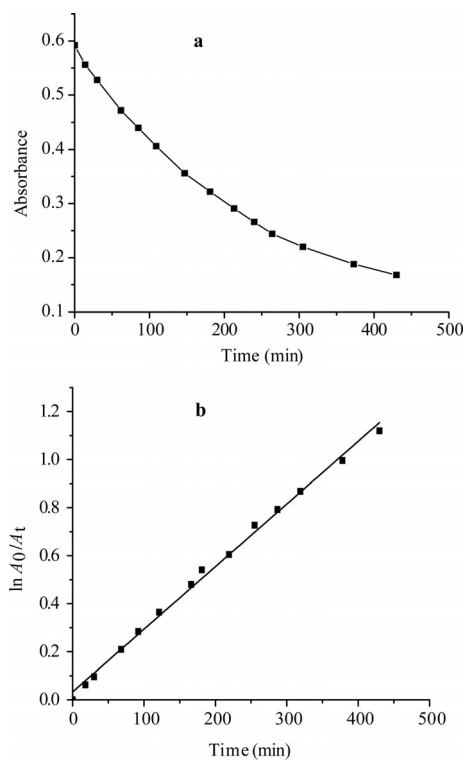
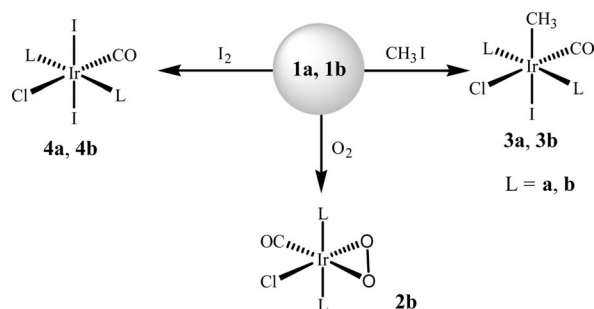


Figure 5. [a] Kinetic plot for **1b** showing the decay of the UV/Vis band at $\lambda_{\text{max}} = 382.5\text{ nm}$ during the reaction of **1b** with molecular O_2 . [b] Plot of $\ln(A_0/A_t)$ vs. time for the reaction of **1b** with molecular O_2 at $25\text{ }^\circ\text{C}$.

that obtained by UV/Vis spectroscopy. The rate of dioxygen addition towards Vaska's complex was also measured by UV/Vis spectroscopy and the rate constant was found to be $9.1 \times 10^{-4} \text{ s}^{-1}$, which reveals that the rate of dioxygen addition in **1b** is about three times faster than that of Vaska's complex and this enhanced reactivity may be due to the higher nucleophilicity of the iridium centre in the former.

Reactivity of **1a** and **1b** with CH_3I and I_2

Complexes **1a** and **1b** are coordinatively unsaturated and undergo OA reactions with different electrophiles like CH_3I and I_2 to afford six-coordinate Ir^{III} complexes of the type *trans*- $[\text{Ir}(\text{CO})(\text{CH}_3)\text{ClL}_2]$ (**3a**, **3b**) and *trans*- $[\text{Ir}(\text{CO})\text{I}_2\text{L}_2]$ (**4a**, **4b**) (Scheme 2). The IR spectra of all the complexes in CHCl_3 show a single intense terminal $\nu(\text{CO})$ absorption in the range $2040\text{--}2063 \text{ cm}^{-1}$ indicating the formation of the oxidised Ir^{III} products. The ^1H NMR spectra of **3a** and **3b** show a singlet at around $\delta = 3.09\text{--}3.12$ ppm for the methyl proton of the $\text{Ir}\text{--}\text{CH}_3$ group and other characteristic bands for $\text{COOCH}_3/\text{OCH}_3$ and phenylic protons are obtained in their respective ranges. The ^1H NMR spectra of **4a** and **4b** do not show any major changes in their chemical shifts compared to the parent complexes (**1a**, **1b**). ^{31}P NMR spectra of each of the complexes **3a**, **3b**, **4a** and **4b** exhibit characteristic $^{31}\text{P}\{^1\text{H}\}$ NMR resonances in the range $\delta = 1.5\text{--}4.3$ ppm, and the ^{13}C NMR spectra show different characteristic resonances for terminal CO in the range $\delta = 182.3\text{--}186.4$ ppm, methyl carbon atoms in the range $\delta = 48.3\text{--}58.5$ ppm and phenylic carbon atoms in the range $\delta = 122.5\text{--}141.3$ ppm.



Scheme 2. Oxidative addition of different electrophiles towards **1a** and **1b**.

Conclusions

Two new Vaska-type complexes **1a** and **1b** have been synthesised and characterised, which undergo oxidative addition with small molecules like CH_3I and I_2 to produce Ir^{III} carbonyl species *trans*- $[\text{Ir}(\text{CO})(\text{CH}_3)\text{ClL}_2]$ (**3a**, **3b**) and *trans*- $[\text{Ir}(\text{CO})\text{I}_2\text{L}_2]$ (**4a**, **4b**). The X-ray crystal structure of **1a** shows long-range "secondary" $\text{Ir}\cdots\text{O}$ bonding. Complex **1a** is found to be inert towards dioxygen addition; on the other hand, **1b** reacts rapidly with O_2 to generate **2b**. The kinetic study of the reaction of **1b** and Vaska's complex

towards dioxygen addition revealed that the rate of dioxygen addition to **1b** is about three times faster than for Vaska's complex.

Experimental Section

General: All operations were carried out under nitrogen. All solvents were distilled under N_2 prior to use. $\text{IrCl}_3 \cdot x\text{H}_2\text{O}$ was purchased from M/S Arora Matthey Ltd., Kolkata.

Elemental analyses were performed with a Perkin–Elmer 2400 elemental analyser. UV/Vis spectra were recorded with a UV/Vis spectrophotometer model Shimadzu 1610 PC. IR spectra ($4000\text{--}400 \text{ cm}^{-1}$) were recorded in CHCl_3 solution and nujol with a Perkin–Elmer system 2000 FT-IR spectrophotometer. The ^1H , ^{13}C and ^{31}P NMR spectra were recorded in CDCl_3 solution with a Jeol Delta 270 MHz spectrometer at room temperature (r.t.) and chemical shifts were reported relative to SiMe_4 and 85% H_3PO_3 as internal and external standards, respectively.

Synthesis of the Ligands 2-Ph₂PC₆H₄COOCH₃ (a) and 2-Ph₂PC₆H₄OCH₃ (b): The ligands were prepared according to literature methods.^[19]

Synthesis of the Starting Complex $[\text{Ir}(\text{COE})_2\text{Cl}]_2$ (COE = *cis*-cyclooctene): The starting complex $[\text{Ir}(\text{COE})_2\text{Cl}]_2$ was prepared by refluxing $\text{IrCl}_3 \cdot x\text{H}_2\text{O}$ and *cis*-cyclooctene in 2-propanol for about 3 h under nitrogen.^[20]

Synthesis of the Complexes *trans*- $[\text{Ir}(\text{CO})\text{Cl}(\text{2-Ph}_2\text{PC}_6\text{H}_4\text{COOMe})_2]$ (1a**) and *trans*- $[\text{Ir}(\text{CO})\text{Cl}(\text{2-Ph}_2\text{PC}_6\text{H}_4\text{OMe})_2]$ (**1b**):** $[\text{Ir}(\text{COE})_2\text{Cl}]_2$ (0.223 mmol, 200 mg) was dissolved in acetonitrile. The solution was then stirred at r.t. for about 10 min under a nitrogen atmosphere. After that the flow of N_2 was stopped and CO gas was passed to the solution until a clear greenish yellow solution was obtained. A stoichiometric amount ($\text{Ir}/\text{ligand} = 1:2$) of the ligand [0.897 mmol, 287 mg (**a**), 262 mg (**b**)] in DCM was then added to the solution and the mixture was stirred for about another 30 min. The solvent was evaporated under vacuum and washed with diethyl ether. The bright yellow compound thus obtained was recrystallised from DCM/hexane and stored over silica gel in a desiccator.

Analytical Data for **1a:** Yield 90%. IR: $\tilde{\nu} = 1940$ (nujol), 1957 (CHCl_3) $[\nu(\text{CO})]$, 1721 $[\nu(\text{COOCH}_3)] \text{ cm}^{-1}$. ^1H NMR (CDCl_3): $\delta = 3.47$ (s, 6 H, COOCH_3), 7.34–8.21 (m, 28 H, Ph) ppm. ^{13}C NMR (CDCl_3): $\delta = 51.76$ (s, CH_3), 126.3–135.8 (m, Ph), 166.98 (s, CO_{ester}), 181.3 (s, CO_t) ppm. ^{31}P NMR (CDCl_3): $\delta = 28.97$ (s, 1 P) ppm. $\text{C}_{41}\text{H}_{34}\text{ClIrO}_5\text{P}_2$ (895.7): calcd. C 54.93, H 3.79; found C 54.78, H 3.71.

****1b**:** Yield 88%. IR (CHCl_3): $\tilde{\nu} = 1942$ (nujol), 1959 (CHCl_3) $[\nu(\text{CO})] \text{ cm}^{-1}$. ^1H NMR (CDCl_3): $\delta = 3.59$ (s, 6 H, OCH_3), 6.83–7.95 (m, 28 H, Ph) ppm. ^{13}C NMR (CDCl_3): $\delta = 55.8$ (s, CH_3), 123.3–138.6 (m, Ph), 168.3 (s, C–O Ph), 180.1 (s, CO_t) ppm. ^{31}P NMR (CDCl_3): $\delta = 19.49$ (s, 1 P) ppm. $\text{C}_{39}\text{H}_{34}\text{ClIrO}_5\text{P}_2$ (839.7): calcd. C 55.73, H 4.05; found C 55.58, H 3.97.

Synthesis of *trans*- $[\text{Ir}(\text{O}_2)(\text{CO})\text{ClL}_2]$ (2b**):** Complex **1b** (100 mg) was dissolved in DCM (25 cm^3) and the solution was then placed into a 50 mL beaker. The reaction mixture was stirred at r.t. and air was passed into the mixture for about 6 h to allow dioxygen uptake. The solvent was evaporated under vacuum and the orange compound so obtained was recrystallised from hexane/DCM and stored over silica gel in a desiccator.

However, **1a** does not react with molecular oxygen under similar experimental conditions.

Analytical Data for 2b: IR (CHCl₃): $\tilde{\nu}$ = 2011 [v(CO)], 858 [v(O–O)] cm⁻¹. ¹H NMR (CDCl₃): δ = 3.71 (s, 6 H, OCH₃), 7.03–7.79 (m, 28 H, Ph) ppm. ¹³C NMR (CDCl₃): δ = 56.3 (s, CH₃), 122.8–139.3 (m, Ph), 170.3 (s, C–O_{Ph}), 180.8 (s, CO_I) ppm. ³¹P NMR (CDCl₃): δ = 1.52 (s, 1 P) ppm. C₃₉H₃₄ClIrO₅P₂ (871.7): calcd. C 53.69, H 3.90; found C 53.50, H 3.89.

Synthesis of [Ir(CO)(CH₃)ClL₂] (3a, 3b) [L = 2-Ph₂PC₆H₄COOMe (a), 2-Ph₂PC₆H₄OMe (b)]: [Ir(CO)ClL₂] (100 mg) was dissolved in DCM (15 cm³) and to that solution CH₃I (6 cm³) was added. The reaction mixture was then stirred at r.t. for about 10 min. The solution changed from yellow to orange and the solvent was evaporated under vacuum. The compound so obtained was washed with diethyl ether and stored over silica gel in a desiccator.

3a: IR (CHCl₃): $\tilde{\nu}$ = 2042 [v(CO)] cm⁻¹. ¹H NMR (CDCl₃): δ = 3.12 (s, 3 H, CH₃), 3.63 (s, 6 H, -COOCH₃), 7.05–8.16 (m, 28 H, Ph) ppm. ¹³C NMR (CDCl₃): δ = 48.3, 53.6 (s, CH₃), 125.8–138.3 (m, Ph), 165.8 (s, CO_{ester}), 184.9 (s, CO_I) ppm. ³¹P NMR (CDCl₃): δ = 2.6 (s, 1 P) ppm. C₄₂H₃₇ClIrO₅P₂ (1037.6): calcd. C 48.56, H 3.57; found C 48.08, H 3.48.

3b: IR (CHCl₃): $\tilde{\nu}$ = 2040 [v(CO)] cm⁻¹. ¹H NMR (CDCl₃): δ = 3.09 (s, 3 H, CH₃), 3.78 (s, 6 H, -OCH₃), 6.97–7.83 (m, 28 H, Ph) ppm. ¹³C NMR (CDCl₃): δ = 49.6, 58.5 (s, CH₃), 122.5–139.4 (m, Ph), 171.3 (s, C–O_{Ph}), 182.3 (s, CO_I) ppm. ³¹P NMR (CDCl₃): δ = 1.5 (s, 1 P) ppm. C₄₀H₃₇ClIrO₅P₂ (981.6): calcd. C 48.90, H 3.77; found C 48.62, H 3.69.

Synthesis of [Ir(CO)Cl₂L₂] (4a, 4b): [Ir(CO)ClL₂] (100 mg) was dissolved in DCM (15 cm³) and to that solution I₂ (50 mg) was added. The reaction mixture was then stirred at r.t. for about 2 h. The solvent was evaporated under vacuum and the brown compound so obtained was washed with hexane several times and stored over silica gel in a desiccator.

4a: IR (CHCl₃): $\tilde{\nu}$ = 2063 [v(CO)] cm⁻¹. ¹H NMR (CDCl₃): δ = 3.53 (s, 6 H, COOCH₃), 7.21–8.14 (m, 28 H, Ph) ppm. ¹³C NMR (CDCl₃): δ = 52.3 (s, CH₃), 128.5–141.3 (m, Ph), 165.8 (s, CO_{ester}), 186.4 (s, CO_I) ppm. ³¹P NMR (CDCl₃): δ = 4.3 (s, 1 P) ppm. C₄₁H₃₄Cl₂IrO₅P₂ (1149.5): calcd. C 42.80, H 2.96; found C 42.54, H 2.89.

4b: IR (CHCl₃): $\tilde{\nu}$ = 2060 [v(CO)] cm⁻¹. ¹H NMR (CDCl₃): δ = 3.79 (s, 6 H, OCH₃), 6.93–7.89 (m, 28 H, Ph) ppm. ¹³C NMR (CDCl₃): δ = 55.9 (s, CH₃), 124.2–139.5 (m, Ph), 168.5 (s, C–O_{Ph}), 185.9 (s, CO_I) ppm. ³¹P NMR (CDCl₃): δ = 3.5 (s, 1 P) ppm. C₃₉H₃₄Cl₂IrO₅P₂ (1093.5): calcd. C 42.80, H 3.11; found C 42.35, H 3.03.

X-ray Structural Analysis: Single crystals of **1a** and **2b** were grown by layering a CH₂Cl₂ solution of **1a** and **2b** with n-hexane. The intensity data for the compounds were collected with a Rigaku Saturn CCD using Mo-K α radiation (λ = 0.71073 Å) at 125 K. The structures were solved with SHELXS-97 and refined by full-matrix least-squares on F² using the SHELXL-97 computer program.^[21] Hydrogen atoms were idealised by using the riding models.

CCDC-737947 (for **1a**) and -755360 (for **2b**) contain the supplementary crystallographic data for this paper. These data can be obtained free of charge from the Cambridge Crystallographic Data Centre via www.ccdc.cam.ac.uk/data_request/cif.

Kinetic Experiment: Kinetic experiments of the OA reaction of complexes **1b** and Vaska's complex with dioxygen were carried out using UV/Vis and FTIR spectroscopy in a solution cell. In order to obtain the pseudo-first-order condition, a dilute solution of the complexes (4 × 10⁻⁴ M) was prepared in toluene. 50 cm³ of the stock solution was placed in a 100 mL beaker and the solution was stirred in an open atmosphere to allow dioxygen uptake. Measurements were

made after a regular interval of time by UV/Vis spectroscopy in the region 600–300 nm. After completion of the experiment, absorbance vs. time data for the decay of an appropriate wavelength (λ_{\max} = 380–390 nm) were analysed offline using OriginPro 7.5 software. The pseudo-first-order rate constants were determined from the gradient of the plot of ln(A₀/A_t) vs. time, where A₀ is the initial absorbance and A_t is the absorbance at time t.

In order to correlate the results obtained from the UV/Vis spectra, the kinetic experiment was again carried out with FTIR spectroscopy. FTIR spectra (4.0 cm⁻¹ resolution) were scanned in the v(CO) region (2200–1600 cm⁻¹) and saved at regular time intervals using the spectrometer software. Kinetic measurements were made by following the decay of the v(CO) bands of the complexes in the region 1955–1965 cm⁻¹. The pseudo-first-order rate constants were determined as mentioned above.

Acknowledgments

The authors are grateful to the Director, North East Institute of Science and Technology (CSIR) Jorhat 785006, Assam, India, for his kind permission to publish this work. The Department of Science and Technology (DST), New Delhi (grant number SR/S1/IC-05/2006), the Royal Society of Chemistry (RSC), UK and the Council of Scientific and Industrial Research (CSIR), India (International Joint Project, 2007/R2-CSIR) are acknowledged for partial financial grants. B. D. and B. J. S. thank the CSIR, New Delhi, for providing Senior Research Fellowships.

- [1] L. Vaska, *Acc. Chem. Res.* **1968**, *1*, 335–344.
- [2] a) G. J. Sunley, D. J. Watson, *Catal. Today* **2000**, *58*, 293–307; b) P. R. Ellis, J. M. Pearson, A. Haynes, H. Adams, N. A. Bailey, P. M. Maitlis, *Organometallics* **1994**, *13*, 3215–3226; c) T. R. Griffin, D. B. Cook, A. Haynes, J. M. Pearson, D. Monti, G. E. Morris, *J. Am. Chem. Soc.* **1996**, *118*, 3029–3030; d) M. Lei, W. Zhang, Y. Chen, Y. Tang, *Organometallics* **2010**, *29*, 543–548; e) R. D. Adams, B. Captain, L. Zhu, *J. Organomet. Chem.* **2008**, *693*, 819–833; f) W. B. Tolman, E. I. Solomon, *Inorg. Chem.* **2010**, *49*, 3555–3556; g) W. B. Tolman, *Activation of Small Molecules*, Wiley-VCH, Weinheim, Germany, **2006**; h) A. J. Muller, J. Conradie, W. Purcell, S. S. Basson, J. A. Venter, *South African J. Chem.* **2010**, *63*, 11–19.
- [3] a) D. Forster, *J. Am. Chem. Soc.* **1976**, *98*, 846–848; b) D. Forster, *Adv. Organomet. Chem.* **1979**, *17*, 255–267; c) D. Forster, T. C. Singleton, *J. Mol. Catal.* **1982**, *17*, 299–303.
- [4] a) G. J. Sunley, D. J. Watson, *Catal. Today* **2000**, *58*, 293–307; b) J. H. Jones, *Platinum Met. Rev.* **2000**, *44*, 94–105.
- [5] a) D. B. Williams, W. Kaminsky, J. M. Mayer, K. I. Goldberg, *Chem. Commun.* **2008**, 4195–4197; b) L. I. Simandi, *Dioxygen Activation and Homogeneous Catalytic Oxidation*, Elsevier, New York, **1991**; c) J.-U. Rohde, M. R. Kelley, W.-T. Lee, *Inorg. Chem.* **2008**, *47*, 11461–11463; d) M. Costas, A. Llobet, *J. Mol. Catal. A* **1999**, *142*, 113–124; e) P. A. Shapley, in: *Activation and Functionalization of C–H Bonds* (Eds.: K. I. Goldberg, A. S. Goldman), chapter 22, ACS Symposium Series 885, **2004**; f) C. Limberg, J. H. Telesb, *Adv. Synth. Catal.* **2001**, *343*, 447–449; g) A. Bakac, *Inorg. Chem.* **2010**, *49*, 3584–3593.
- [6] a) L. Vaska, *Science* **1963**, *140*, 809–810; b) L. Vaska, L. S. Chen, *J. Chem. Soc., Chem. Commun.* **1971**, 1080–1081.
- [7] a) Y. B. Lee, W. T. Wong, *Chem. Commun.* **2007**, 3924–3926; b) L. Vaska, *Acc. Chem. Res.* **1976**, *9*, 175–178.
- [8] H. Lebel, C. Ladjel, F. B. Garipey, F. Schaper, *J. Organomet. Chem.* **2008**, *693*, 2645–2648.
- [9] A. Roodt, S. Otto, G. Steyl, *Coord. Chem. Rev.* **2003**, *245*, 121–137.
- [10] a) N. F. Stuurman, J. Conradie, *J. Organomet. Chem.* **2009**, *694*, 259–268; b) C. E. Johnson, R. Eisenberg, *J. Am. Chem. Soc.*

- 1985, 107, 3148–3160; c) X. Li, T. Vogel, C. D. Incarvito, R. H. Crabtree, *Organometallics* **2005**, 24, 62–76.
- [11] D. K. Dutta, J. D. Woollins, A. M. Z. Slawin, D. Konwar, P. Das, M. Sharma, P. Bhattacharyya, S. M. Aucott, *Dalton Trans.* **2003**, 2674–2679.
- [12] R. Brady, W. H. D. Camp, B. R. Flynn, M. L. Schneider, J. D. Scott, L. Vaska, M. F. Werneke, *Inorg. Chem.* **1975**, 14, 2669–2675.
- [13] a) S. C. Zinner, C. F. Rentsch, E. Herdtweck, W. A. Herrmann, F. E. Kühn, *Dalton Trans.* **2009**, 7055–7062; b) A. A. Bowden, J. D. Atwoot, *J. Coord. Chem.* **1998**, 46, 203–209; c) T. Osswald, H. Ruegger, A. Mezzeti, *Chem. Eur. J.* **2010**, 16, 1388–1397; d) S. Perez, C. Lopez, R. Bosque, X. Solans, M. F. Bardia, A. Roig, E. Molins, P. W. N. M. van Leeuwen, G. P. F. van Strijdonck, Z. Freixa, *Organometallics* **2008**, 27, 4288–4299.
- [14] a) D. K. Dutta, J. D. Woollins, A. M. Z. Slawin, D. Konwar, M. Sharma, P. Bhattacharyya, S. M. Aucott, *J. Organomet. Chem.* **2006**, 691, 1229–1234; b) D. K. Dutta, J. D. Woollins, A. M. Z. Slawin, A. L. Fuller, B. Deb, P. P. Sarmah, M. G. Pathak, D. Konwar, *J. Mol. Catal. A* **2009**, 313, 100–106; c) D. Bora, B. Deb, A. L. Fuller, A. M. Z. Slawin, J. D. Woollins, D. K. Dutta, *Inorg. Chim. Acta* **2010**, 363, 1539–1546; d) B. Deb, P. P. Sarmah, D. K. Dutta, *Eur. J. Inorg. Chem.* **2010**, 1710–1716; e) B. Deb, D. K. Dutta, *J. Mol. Catal. A* **2010**, 326, 21–28.
- [15] J. Blin, P. Braunstein, J. Fischer, G. Kickelbick, M. Knorr, X. Morise, T. Wirth, *J. Chem. Soc., Dalton Trans.* **1999**, 2159–2169.
- [16] E. M. Miller, B. L. Shaw, *J. Chem. Soc., Dalton Trans.* **1974**, 480–485.
- [17] J. S. Valentine, *Chem. Rev.* **1973**, 73, 235–245.
- [18] B. L. Shaw, R. E. Stainbank, *J. Chem. Soc., Dalton Trans.* **1972**, 223–228.
- [19] a) B. M. Trost, D. L. V. Vranken, C. Bingel, *J. Am. Chem. Soc.* **1992**, 114, 9327–9343; b) H. K. Reinius, R. H. Latinen, A. O. I. Krause, J. T. Puriainen, *Catal. Lett.* **1999**, 60, 65–70.
- [20] J. L. Herde, J. C. Lambert, C. V. Senoff, *Inorg. Synth.* **1974**, 15, 18–20.
- [21] G. M. Sheldrick, *Acta Crystallogr., Sect. A* **2008**, 64, 112–122.

Received: September 20, 2010
Published Online: January 12, 2011